MEDWIN PUBLISHERS
Committed to Create Value for Researchers

Nanomedicine & Nanotechnology Open Access
ISSN: 2574-187X

Review on the Novel Routes for Preparation of Advanced Nanomaterials for Removal of Organic Dyes from Aqueous Solution

Abd-Elhamid AI*

Advanced Technology and New Materials Research Institute, Egypt

***Corresponding author:** Abd-Elhamid AI, Advanced Technology and New Materials Research Institute, City of Scientific Research and Technological Applications (SRTA-City), New Borg Al-Arab, Alexandria 21934, Egypt, Email: ahm_ch_ibr@yahoo.com

Review Article

Volume 6 Issue 1

Received Date: February 01, 2021

Published Date: March 10, 2021

DOI: 10.23880/nnoa-16000209

Abstract

Organic dyes are considered from most commonly industrial effluents that discharged in raw water. However, the presence of these materials in the water has a harmful effect on the living organism. Therefore, great efforts have been carried out for efficient remove of these toxic dyes from the contaminated water. Recently, the nanotechnologies have highly developed, which presented an enhanced opportunity for improving innovative methods for preparation of efficient nanomaterials that offer a satisfied removal of dyes from wastewater simply and with a low-cost. These strategies provide (large surface area, modified surface properties, unique electron conduction properties, etc.) nanomaterials with excellent performances in eliminating of toxic dyes wastewater.

Keywords: Nanomaterials; Organic Dyes

Abbreviations: IONs: Iron-Based Nanomaterials; SPIONs: Superparamagnetic Iron Oxide Nanoparticles; PEI: Poly-Ethyleneimine; BPB: Bromophenol Blue; BCG: Bromocresol Green; RhB: Rhodamine B; MB: Methylene Blue; CCD: Central Composite Design; MAH: Maleic Anhydride; BHHPs: Biobased Hydrolyzed Hollow Particles; MO: Methyl Orange; GO: Graphene Oxide; COF: Covalent Organic Frameworks; BN: Boron Nitride; CV: Crystal Violet; OG: Orange G; MOF: Metal-Organic Framework; AC: Activated Carbon; OMC: Ordered Mesoporous Carbons; MC: Mesoporous Carbons; MWCNTs: Multiwalled Carbon Nanotubes; MG: Malachite Green; PIL: Poly Ionic Liquids; PDA: Polydopamine; DA: Dopamine; SY: Sunset Yellow; CST: Cationic Starches; CCQM: Cationic Polyelectrolyte Microsphere; PCM: Pure Chitosan Microsphere; MG: Malachite Green; PES: Polyethersulfone; NF: Nanofiltration; PWF: Pure Water Flux; CS: Corn Stalks; CCL: Cinnamomum Camphora Leave; CCSD: Cinnamomum Camphora Saw Dust; LCST: Lower Critical Solution Temperature.

Introduction

Nowadays, the contamination of water by different toxic species such as organic pollutants attracts high attention [1]. Examples of these effluents, organic dyes are often exhausts into the raw-water from dye manufacturing such as; paper making, printing, leather, textile industries, painting, etc. These organic species difficultly to be biodegraded naturally and resulted in great harmful to living organisms. Adsorption-based wastewater treatment strategy is one of the most popular techniques for remediation of wastewater to sequester and eliminate toxic dyes from the polluted water, which has several advantages like as; high efficiency, low cost and easy to setup [2-4]. For this approach, the selection of suitable adsorbents is of very importance for achieving the appropriated results.

Adsorbent	Adsorbate	q^o mg g^{-1}	Ref.
phosphate capped $CoFe_2O^4$ NPs	Methylene blue	4.5	[17]
PEI-coated SPIONs	bromophenol blue	15.5	[18]
	bromocresol green	11.3	
Fe_3O_4@PDA/CMC	methylene blue	217.43	[19]
	crystal violet	262.27	
	methyl orange	83.47	
	congo red	92.83	
Ni@GO@CNT	rhodamine B	41.5	[20]
mesoporous silica powder	methylene blue	135	[21]
SiO_2-BHHPs	methyl orange	701	[22]
$Mg_2Si_3O_6(OH)_4$/GO nanocomposite	methylene blue	909.1	[23]
NCS-NiS	methylene blue	1006.52	[24]
	crystal violet	1946.61	
{[Zn (1,3-BDC)L]·H2O}n	Amido Black 10 B	2402.82	[25]
	Methyl Orange	744.02	
	Orange II	522.83	
	Direct Red 80	1496.34	
MWCNTs/AC	methylene blue	232.5	[26]
	methyl orange	196.1	
S-CS@TB	Malachite Green	53.35	[27]
	Rhodamine B	40.86	
OMC	Acid Violet 90	1311.5	[28]
MC	Congo red	331.49	[29]
H-PDA-MCs	methylene blue	191.55	[30]
PQAM	methyl orange	909.8	[31]
PDVIm-Cl	acid orange 7	1808 ± 84	[32]
	sunset yellow 19	1022 ± 8	
	reactive blue	2605 ± 254	
	congo red	6930 ± 196	
Mt-CST11 and Mt-CST21	Basic Yellow	333.3	[33]
CCQM	Congo red	1500	[34]
	Methyl orange	179.4	
CTS-HMP	malachite green Reactive Red–195	69.4	[35]
		148	
M-CS,	methylene blue	870	[36]
M-CCL		741	
M-CCSD		787	
0.05GO/PNIPAM	Rhodamine B	982	[37]

Table 1: different adsorbent based nanomaterials, adsorbed organic dyes and maximum adsorption capacities.

Nanomaterials have received great attention due to their various physico-chemical features like the surface area to volume ratio, chemical reactivity, optical and electronic properties from that of bulk materials [5-7]. The composition, size, shape, structure and dimension of a nanomaterial greatly based on the preparation strategy. Moreover, the adsorption behavior of a nanomaterial can be varied by the stoichiometric ratio of reactants, reaction temperature, capping agents/surfactants and pH of the reaction [8-12]. On the other hand, the adsorption of adsorbate on the

nanomaterials can take place via different mechanisms such as electrostatic interaction, hydrogen bonding, surface/pore diffusion, coordination effect and hydrophobic interaction [13-16]. Additionally, the functionalization of surface charge can be done with the aid of functional groups on the surface to enhance the adsorption of a particular type of dyes. Here in we will discuss various innovated strategies for preparation of preformed adsorbent based nanomaterials for removal of colored organic dyes. Table 1, presents different adsorbent based nanomaterials.

Magnetic Based Nanomaterials

Magnetic separation is a low-cost and preformed strategy for recovering adsorbent from the adsorbing media through using of an external magnetic field. Fe_3O_4 nanoparticles (Fe_3O_4 NPs) have been usually used in designing of magnetic materials required for removing dyes due to its good magnetic functions, large specific surface area, low cost, biocompatibility, chemical stability, and easy synthesis [38]. However, magnetic nanoparticles tend to loss its magnetic properties and aggregate in aqueous solution attributed to their large surface energies and magnetic attractive forces [39.]. Therefore, great efforts have been carried out to modify the magnetic nanoparticles surface with a functional layer to enhance its dispensability and removing efficiency.

Iron-based nanomaterials (IONs-1 and IONs-2) were prepared and characterized from zero-valent iron nanoparticles (IONs-0) by Cruz, et al. [40]. Where, IONs-1 was fabricated from IONs-0 by hydrogen peroxide exposure then calcination at 350 ◦ C. While, IONs-2 was fabricated from IONs-0 by using both hydrogen peroxide and sodium hydroxide, respectively. The obtained data showed that, IONs-1 (nanorods) exhibited the following phases: superparamagnetic Fe^{3+} (7%), α-Fe_2O_3 (17%), and γ- Fe_2O_3 (76%) and IONs-2 (nanosheets) with phase composition: superparamagnetic Fe^{3+} (5%), γ-Fe_2O_3 (51%) and Fe_3O_4 (54%) and the specific surface areas of IONs-1 (85.37 m^2 g^{-1}) and IONs-2 (223.84 m^2 g^{-1}). Finally, the IONs-1 and IONs-2 were employed to eliminate Direct Red 80 dye from aqueous solution.

Cobalt ferrite nanoparticles grafted with an ultrathin phosphate layer of ~ 1 nm thick were prepared by coprecipitation subsequent by hetero condensation of free surface OH- groups of $CoFe_2O_4$ particles with orthophosphoric acid [17]. The signature of P–O–M stretching vibrations at 900 – 1200 cm^{-1} was confirmed with FTIR. The phosphate moieties capped cobalt ferrite highly improved the adsorption of methylene blue where the adsorption efficiency (~ 89.5 %) and adsorption capacity (~ 4.5 mg. g^{-1}) within 5 min. contact time, as compared to nearly zero related to unmodified $CoFe_2O_4$. These findings show that the adsorption the dye molecule based on functional moieties capped these particles, see Figure 1.

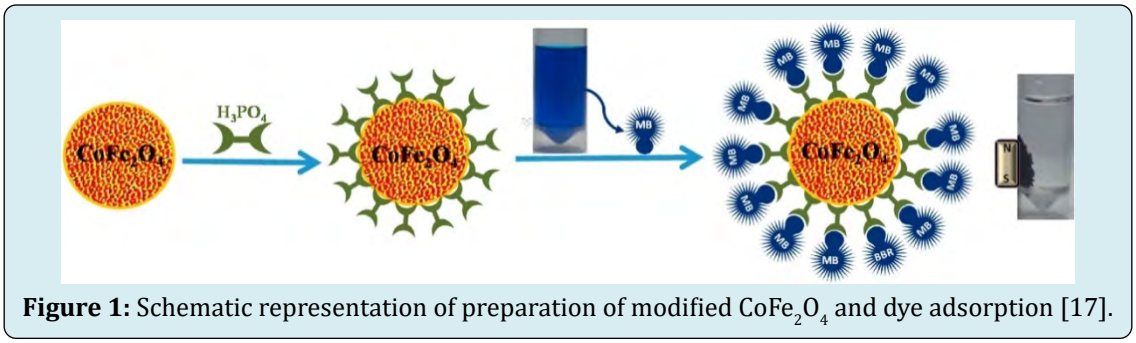

Figure 1: Schematic representation of preparation of modified $CoFe_2O_4$ and dye adsorption [17].

Magnetic carbon nanomaterials were synthesis via a simple one-step hydrothermal route using glucose (carbon sources) and ferric ammonium citrate (iron sources) [41]. Results cleared that, the morphology as-fabricated magnetic nanomaterials are sphere particles with aggregation phase and magnetic Fe-particles are coated by carbon matrixes. In addition, as the calcination temperature, the aggregation degree of the sample decrease, whereas the average particle sizes, BET specific surface areas and saturation magnetizations enhanced. The carbon with graphite structure has higher removal efficiency than that belongs to amorphous carbon for organic dye rhodamine B in water. Moreover, the iron with amorphous structure presented higher photocatalytic activity than that of the iron with crystalline structure for the degradation of rhodamine B. The combination of adsorption and photocatalysis will completely degraded rhodamine B in water.

Matrix-dispersed superparamagnetic iron oxide nanoparticles (SPIONs) were prepared for the elimination of anionic dyes from wastewater exhausted from textile industrial plants [18]. The matrix-dispersed SPIONs were prepared by a solvothermal approach in which a polyethyleneimine (PEI) shell was anchored onto SPIONs in order to create positive charges to their surfaces for adsorption of anionic dyes; bromophenol blue (BPB) and bromocresol green (BCG). It was showed that the uptake capacity of PEI-modified SPIONs is 15.5 mg/g (BCG) and 11.3

mg/g (BPB).

A novel and simple route for preparation of magnetic carboxymethyl chitosan aerogel (Fe_3O_4@PDA/CMC) (Figure 2) has been investigated with the cooperation of mussel-inspired chemistry and Schiff base reaction to adsorb cation and anion dyes [19]. The prepared composite exhibited good adsorption capacity of cationic dye (methylene blue (217.43 mg g^{-1}) and crystal violet (262.27 mg g^{-1})) and anionic dye (methyl orange (83.47 mg g^{-1}) and congo red (92.83 mg g^{-1})). Moreover, the designed magnetic aerogel presented an appropriated recyclability and removal efficiency after seven adsorption-desorption cycles.

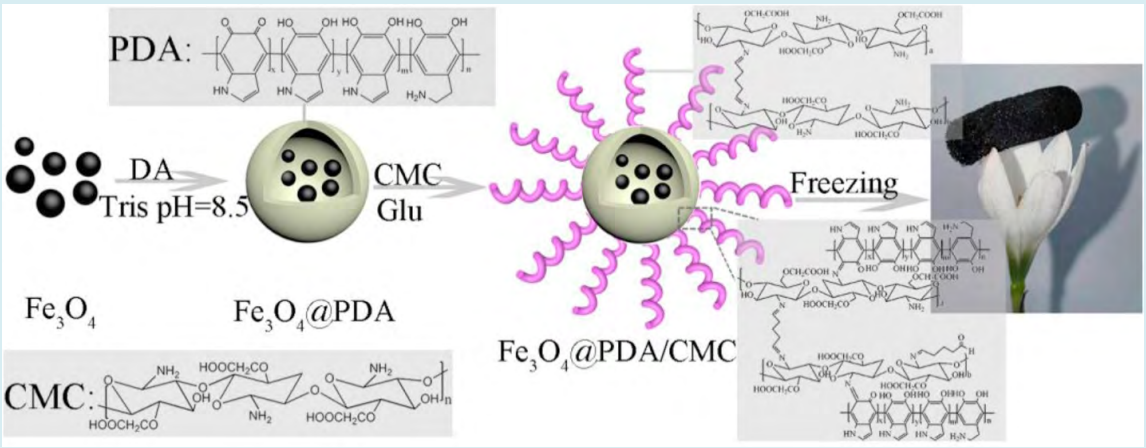

Figure 2: Schematic illustration of the preparation of Fe_3O_4@PDA/CMC aerogel [19].

The nickel nanoparticles anchored graphene oxide-carbon nanotubes nanocomposite was fabricated, as shown in Figure 3, via a novel molecular-level-mixing strategy subsequent by a freeze-drying and then reduction process [20]. The obtained composite exhibit a well-dispersed 3D structure and demonstrated high performance in adsorbing Rhodamine B (RhB) from the aqueous solution via a synergistic effect of physical adsorption and photodegradation. The nanocomposite enclosed 30 wt% of Ni demonstrated the greater removal ability (41.5 mg g^{-1}). Moreover, due to the ferromagnetism of Ni nanoparticles, the nanocomposite could be simply recovered and recycled after the removal of dye via magnetic separation.

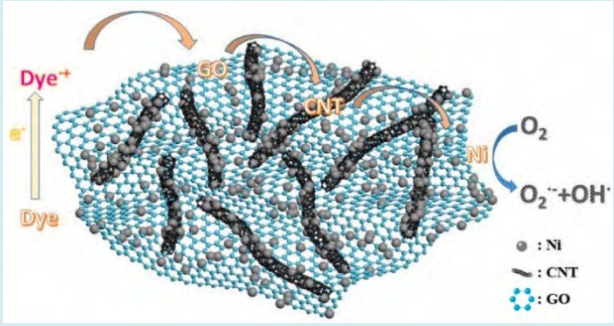

Figure 3: A proposed schematic of the removal mechanism with FGNi nanocomposites [20].

Silica Based Nanomaterials

Silica or silicon dioxide found an especial attention because of surface reactivity derived from silanol (Si–OH) groups, these groups will generate a negative charge on the silica nanoparticles which improve the removal of cationic species. Moreover, the Si-OH groups' facile modification with various active groups to wide their application in different fields.

The amorphous silica with high surface area was prepared for adsorption of the methylene blue (MB) [21]. In the first, the zeolite compounds were prepared hydrothermally from the conversion of a low grade kaolin, containing quartz by varying parameters such as; NaOH concentration, temperature, and reaction time depending on the central composite design method (CCD). Secondly, the mesoporous silica powders were produced by the acid treatment of prepared zeolite compounds at 80^0C. The produced SiO_2 own average pore size (4.3 nm), and specific surface area (637 m^2 g^{-1}) which provided a great number of surface functional groups, leading to the strong chelating with MB in the neutral condition with adsorption capacity of 135 mg g^{-1}. The used adsorbent can be regenerated by thermal treatment without significant changing the adsorption ability.

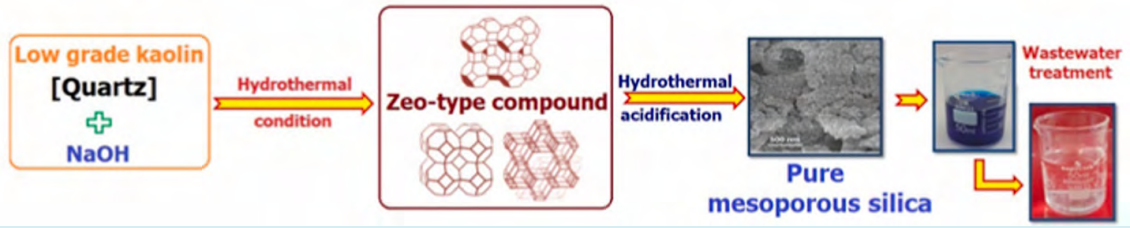

Figure 4: Schematic illustration of the preparation and application of the mesoporous silica [21].

A special type of SiO_2 anchored with biobased hollow polymeric particles was prepared from biomass trans-anethole (ANE) monomers [22]. Initially, The SiO_2 NPs were synthesized using Stober method and functionalized with amino functional groups. In a separated step, the (ANE) monomer and maleic anhydride (MAH) were copolymerized via precipitation polymerization to give hollow polymer particles, which will be hydrolyzed to produce surface carboxyl groups. Finally, the biobased hydrolyzed hollow particles (BHHPs) were reacted with the amino-modified SiO_2 NPs to produce SiO_2-BHHPs, as demonstrated in Figure 5. The studies revealed that, the maximum adsorption capacity toward methyl orange dye (MO) reached up to 701 mg/g and the SiO_2-BHHPs can be easily recycled and reused.

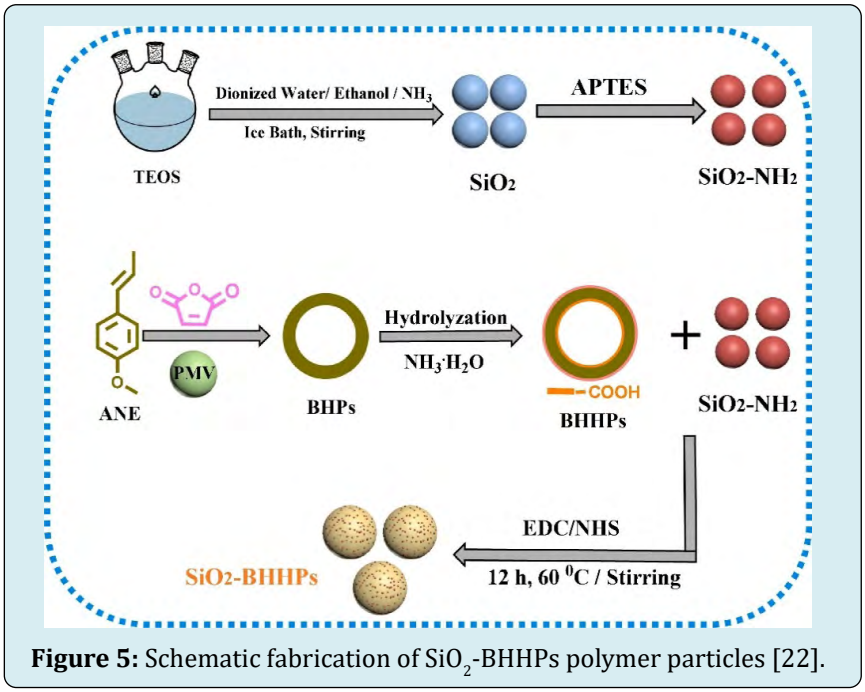

Figure 5: Schematic fabrication of SiO_2-BHHPs polymer particles [22].

Keggin-type heteropoly acids $H_3PMo_{12}O_{40}$ (PMo_{12}), $H_3PW_{12}O_{40}$ (PW_{12}) and $H_4SiW_{12}O_{40}$ (SiW12) were successfully loaded on silica-anchored perovskite type $LaMnO_3$ nanoparticles via a simple acid–base reaction [42] and these innovated hybrid nanomaterials (named as $LaMnO_3$@SiO_2/PMo_{12} (1), $LaMnO_3$@SiO_2/PW_{12} (2), and $LaMnO_3$@SiO_2/SiW_{12} (3)). Furthermore, the adsorption performance of 1–3 were studied towards cationic methylene blue (MB) and anionic methyl orange (MO) dyes. The results presented that the removal percent of MB dye reached to (≥98%) by adsorbents 1–3 in 1, 30 and 0.5 minutes, respectively. Moreover, the as-prepared nanomaterials 1–3 could be reused several times without any influence on their adsorption efficiency and structures.

A novel uniform hollow mesoporous magnesium silicate $Mg_2Si_3O_6(OH)_4$ micro-nanosphere assembled nanosheets has been fabricated by controlling the quantity of silica through the hydrothermal reaction [23]. Thereafter, graphene oxide (GO) was required as a support to produce $Mg_2Si_3O_6(OH)_4$/GO nanocomposite as seen in Figure 6. The GO prevent the agglomeration of $Mg_2Si_3O_6(OH)_4$ and provides extra available adsorption active sites. This nanocomposite provided excellent selective adsorption capacity for MB (909.1 mg/g) and good recyclable behavior.

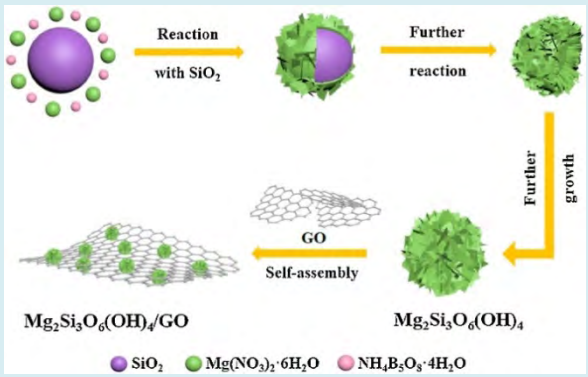

Figure 6: The formation mechanism for $Mg_2Si_3O_6(OH)_4$/GO [23].

Other Nanocomposite

2D nanomaterials have appropriated morphology with excellent physical and chemical behavior making these materials suitable support for the other nanomaterials which making it attractive for research and industrial applications. Abdellaha, et al. [43] investigated one-pot preparation of the composite of covalent organic frameworks (COF) and two-dimensional (2D) nanomaterials (graphene oxide (GO), graphitic carbon nitride (g-C_3N_4), and boron nitride (BN)). Melamine is poly-condensed with terephthaldehyde in the existence of GO, gC_3N_4, and BN result in the yielding of a series of highly cross-linked microporous hierarchical porous amine networks as illustrated in Figure 7. The results showed that, the obtained COF nanocomposites exhibited a high surface area of 42-509 m^2 g^{-1} with a hierarchical porous structure and high thermal decomposition. COF nanocomposites (COF@GO, COF@g-C_3N_4, and COF@BN) were displayed as an efficient adsorbent for dye removal anionic dyes (Eosin dye and fluorescein) and cationic dyes (Fuchsine, and methylene blue).

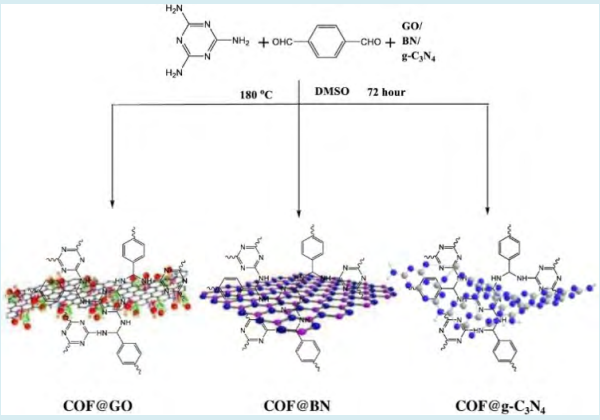

Figure 7: The synthesis procedure of COF and its composite is presented [43].

The modification of surface charge of the nanomaterials with specific functional groups on can enhance the adsorption selectivity of a particular type of dyes. Kumari, et al., [24], were prepared negatively charge surface nickel sulfide nanomaterial via a simple and eco-friendly method using nickel acetate, thioacetamide and L-glutathione reduced (GSH) for dyes and antibiotics removal applications. The nanomaterial presented selective adsorption of the cationic dyes: methylene blue (MB) and crystal violet (CV) with enhance removal capacity of 1006.52 mg g^{-1} and 1946.61 mg g^{-1}, respectively. The selectivity of MB in binary mixtures was explored utilizing two anionic dyes: methyl orange (MO) and orange G (OG). The separation efficiency (α) for MB in MB/MO mixtures was 97.75% and MB/OG mixtures was 99.16 %, as present in Figure 8. The adsorption process for all the adsorbate followed pseudo-second-order kinetics and the Freundlich isotherm model. Moreover, the adsorbent could be reused up to 4 times with 97 % efficiency.

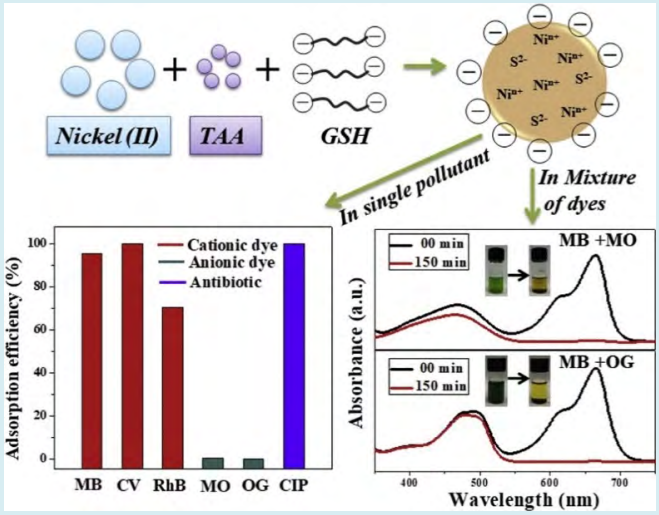

Figure 8: The preparation mechanism of negative nanoparticles and its adsorption of organic dyes [24].

Compared to original porous materials, the chemical and physical features of the Metal-organic frameworks (MOFs) can be developed by careful ligand design, which result in remarkable behavior of extraordinary surface areas, fine-tunable pores as well as adjustable chemical functionality, highly improving the adsorption affinity toward target contaminants. Hydrothermal reaction of $Zn(NO_3)_2.6H_2O$ with a flexible bipyridyl ligand, (pyridin-4-yl)methyl 3-(2-(4- ((pyridin-4-yl)methoxy)phenyl)diazenyl)benzoate (L) and 1,3-benzenedicarboxylic acid (1,3-H2BDC) yield a novel metal-organic framework (MOF), $\{[Zn\ (1,3\text{-}BDC)L]\cdot H_2O\}_n$ [25]. The existence of the ligand L involved ester, diazene and ether groups, numerous of oxygen and nitrogen sites that can be protonated ($N{=}NH^+$, $-OH^+$, $-COOH^+$) in acidic environments were successfully located on the surfaces of the constructed

MOF which will be appropriated for adsorption of anionic dyes from aqueous solutions. Such adsorbent provided ultrahigh uptake capacities for various sized anionic dyes of Amido Black 10 B (AB, 2402.82 mg g^{-1}), Methyl Orange (MO, 744.02 mg g^{-1}), Orange II (OII, 522.83 mg g^{-1}) and Direct Red 80 (DR, 1496.34 mg g^{-1}), see Figure 9. Moreover, the adsorbent presented excellent selectivity in the adsorption of anionic dyes through electrostatic interaction between the protonated Zn-MOF and the anionic dyes.

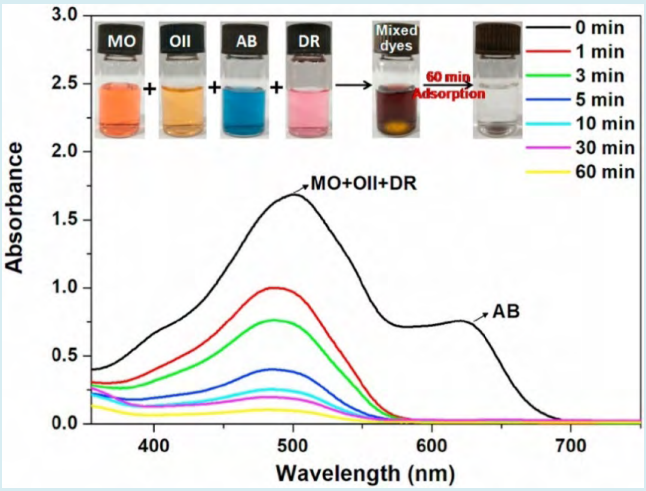

Figure 9: UV–Vis spectral changes of dye mixture in the presence, the inset photographs represent the adsorption process of dyes mixture by using [25].

Carbonaceous Nanomaterials

The superior physicochemical properties and porous structure of carbonaceous nanomaterials do them widely used as adsorbents. Among these materials, activated carbon (AC), multiwalled carbon nanotubes (MWCNTs), biochar, ordered mesoporous carbons (OMC) and mesoporous carbons (MC). Ahlawat, et al. [26], used carbonaceous nanomaterials for adsorptive elimination of methylene blue (MB) and methyl orange (MO) dyes from wastewater under dark conditions Figure 10. The maximum adsorption performance (mg/g) of MB/MO was in the order of MWCNTs/AC nanocomposite (232.5/ 196.1) > MWCNTs (185.1/106.3) > AC (161.3/78.7), this was attributed to the MWCNTs/AC nanocomposite own more active sites on its surface available for adsorption process. Moreover, the MWCNTs/ AC nanocomposite showed high reusable efficiency (90.2%) larger than MWCNTs (81%), and AC (67%) after the first recovery step. Additionally, the availability of these adsorbents was also tested for real field samples.

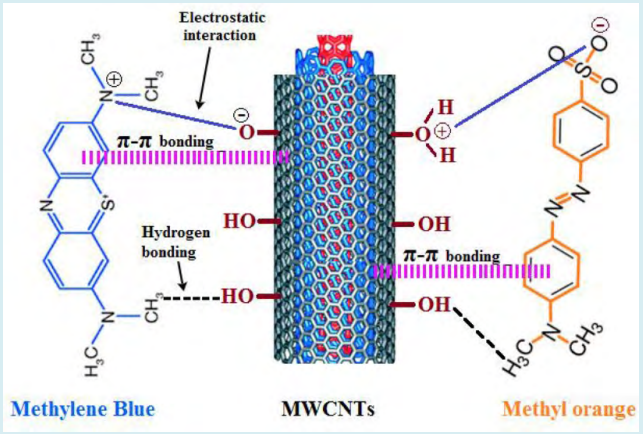

Figure 10: Schematic for the mechanisms of adsorption of both MB and MO dyes onto the MWCNTs [26].

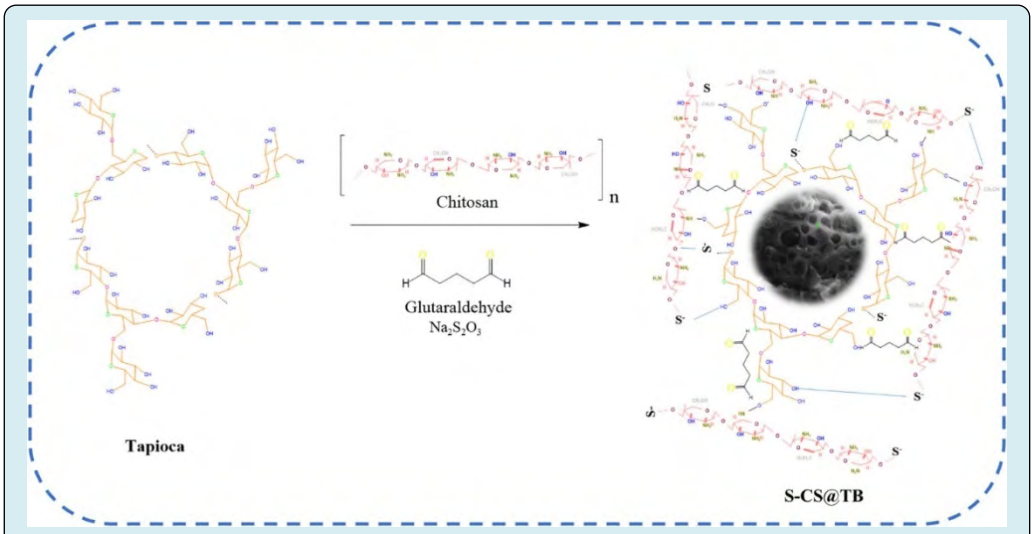

Figure 11: Synthesis route of S-CS@TB composite [27].

A sulfur doped adsorbent of chitosan-tapioca peel biochar (S-CS@TB) composite. Figure 11, was prepared [27] for removal of the organic dyes such as Malachite Green (MG) and Rhodamine B (RhB). The fabricated composite (S-CS@TB) shows the adsorption ability of 53.35 mg/g (MG) and 40.86 mg/g (RhB). Electrostatic attractions, hydrogen bonding and π-π interactions maybe explained the adsorption mechanisms of the dyes over the adsorbent. Finally, the adsorbent could be recovered and reused for five adsorption-desorption cycles.

CMK-8 type ordered mesoporous carbon (OMC) materials were fabricated by hard-templating route using KIT-6 as a mesoporous silica template [28]. Firstly, well-ordered mesoporous KIT-12 sample were obtained through hydrothermal treatment which were used as a templet for preparation of mesoporous carbons. Finally, NaOH solution was applied to leach silica from the silica–carbon matrix and yield mesoporous carbon (C2M1), as presented in Figure 12. The as-prepared nanomaterial showed excellent affinity for anionic Acid Violet 90 (AV 90) with adsorption performance up to 1311.5 mg/g.

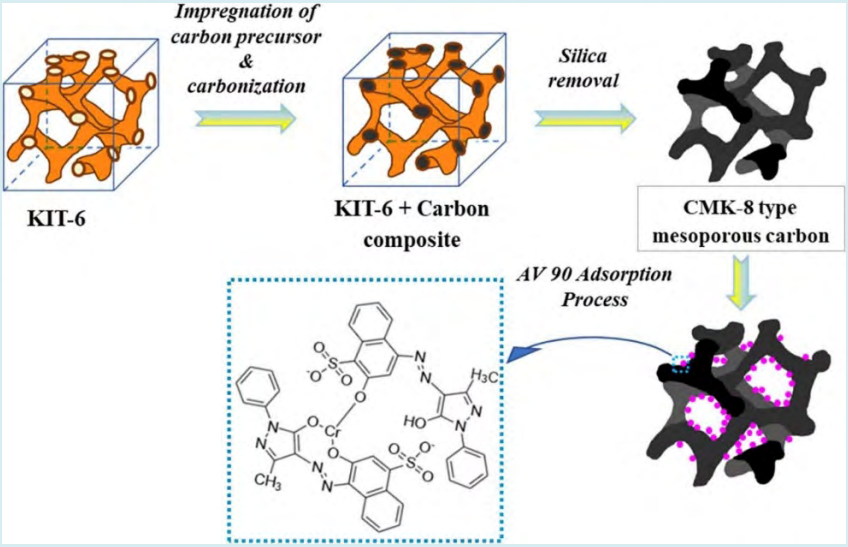

Figure12: Schematic representation of the synthesis of mesoporous carbon material via Hard Template Method using KIT-6 [28].

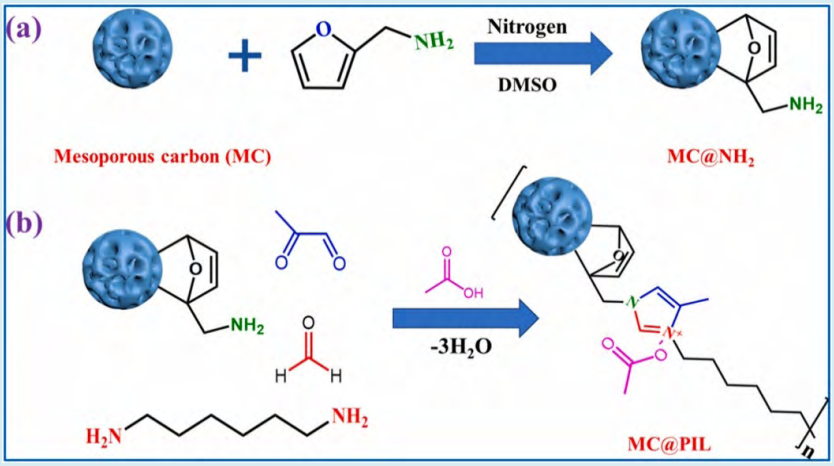

Figure 13: Schematic diagram of preparation of functionalized mesoporous carbon (MC@PIL) via the combination of D–A reaction and Radziszewski reaction [29].

Deng, et al. [29], investigated a novel approach for the surface functionalization of mesoporous carbon (MC) that based on an effective and green Diels-Alder [4+2] cycloaddition and the multicomponent Radziszewski reactions for the first time to in-situ formation poly (ionic liquids) (PIL) on the surface of MC, see Figure 13. Batch

experiments towards adsorbing Congo red (CR) was studied to detect the availability of the prepared composite. The results explored that CR could be fast adsorbed on MC-PIL composites within 10 min with enhancement adsorption performance (331.49 mg/g) towards CR as compared with pristine MC. Additionally, the adsorption/desorption cycle studies of the MC@PIL composites were showed that the adsorption capacity of the third adsorption-desorption cycle can reach 199.0223 mg/g and desorption yield above 80%.

Polydopamine (PDA) is a typical polymer derived by oxide polymerization of dopamine (DA) at ambient temperature in alkaline and aerobic environment. PDA is characterized by presence of various functional groups such as catechol, amine and imine, which enable PDA serve in wide potential applications in the fields of chemistry, biology, medicine and materials science [44,45]. Moreover, PDA could simply assemble on various substrates through in situ self-polymerization of DA [46,47]. Hollow polydopamine microcapsules (H-PDA-MCs) (Figure 14) prepared via a facile oxidation self-polymerization of dopamine using iron trioxide (Fe_2O_3) nano-cube as a template and subjected as a high-efficiency adsorbent for up-taking organic dyes [30]. The experimental results exhibited that H-PDA-MCs provided excellent selective adsorption behavior towards cationic dye with maximum adsorption ability towards MB was up to 191.55 mg g^{-1}.

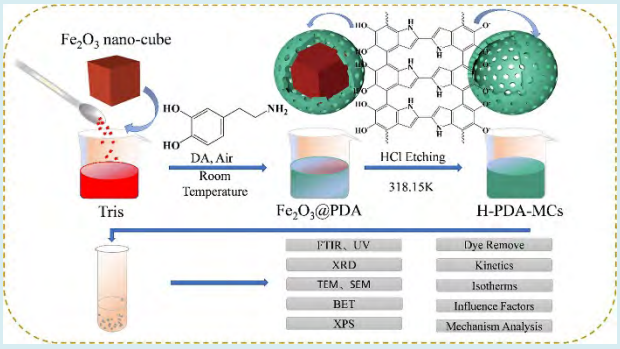

Figure 14: Synthesis and characterization of H-PDA-MCs [30].

The mussel-inspired dopamine (DA), as showed in Figure 15, was employed to functionalized the 3D web-like skeleton of bacterial cellulose (BC) in liquid phase, integrating with 2D graphene oxide (GO) nanosheets to prepare a robust anti-fouling ultrafiltration membrane composite (BC/PDA/RGO) unique superhydrophilicity and underwater superoleophobicity [48]. The as formed bacterial cellulose/polydopamine/reduced graphene oxide composites showed unique superhydrophilicity and underwater superoleophobicity. The composite membrane presented high dye rejection. More interesting, during cycling studies, the membrane manifested superior anti-fouling capability and a high permeate flux recovery ratio (~96.9%) for long-term filtration processes.

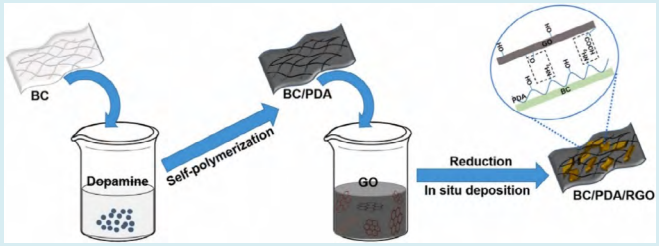

Figure 15: Schematic illustration of bio-inspired fabrication of the BC/PDA/RGO composites [48].

Nanofiber Membranes

The nanofibrous membranes yielded via electrospinning tool have received marked attention as adsorbent nanomaterials for their large specific surface area and high porosity, which provides good performance in water treatment (e.g., dyes removal). Furthermore, electrospinning nanofiber adsorbents could be also constructed to eliminate dyes from wastewater. A poly (methacrylatoethyl trimethyl ammonium chloride-co-methyl methacrylate) copolymer was prepared, and thereafter mixed with polyethersulfone for the synthesis of nanofibrous membranes using electrospinning for fast and enhance removal of dyes and bacteria [31]. Owing to the existence of abundant quaternary ammonium groups, the maximum adsorption quantity for methyl orange was up to 909.8 mg g^{-1}. In addition, the functionalized nanofibrous membranes exhibited good recyclability, selective adsorption performance towards MO, and excellent dynamic removal ability, as shown in Figure 16.

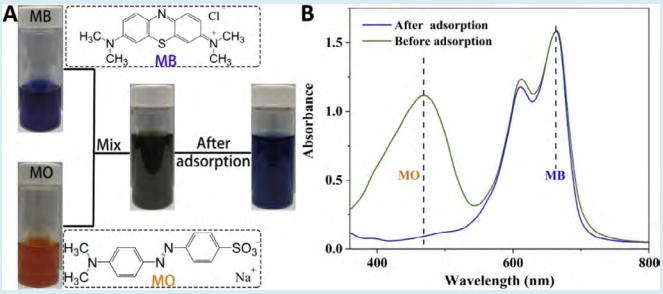

Figure 16: (A) Images of selective adsorption of PQAM for MO from MB/MO mixed solution and the chemical structures of MB and MO; (B) UV–vis spectra of MB/MO mixed solution before and after adsorption [31].

Electrospun fibers composed from nylon 6 was prepared, and employed as a support for laccase loading by adsorption and covalent binding [49]. The systems with

modified laccase were used for decolorization of selected dyes (azo dye Reactive Black 5 and the anthraquinone dye Reactive Blue 4). It was found that the decolorization efficiency of Reactive Blue 4 (77%) and Reactive Black 5 (63%). Moreover, the storage stability studies exhibited that after 30 days' storage, the relative activities were 60% and 95% for adsorbed and covalently bonded oxidoreductase respectively. Furthermore, even after 10 consecutive catalytic cycles adsorbed and covalently modified laccase maintained over 60% and 70%, respectively.

Cationic Organic Polymers

Cationic organic polymers are also examined in the adsorption of anionic dyes by ion exchange with enhanced adsorption amounts. Figure 17, present the preparation of mesoporous poly (N,N' -methylene-bis(1-(3-vinylimidazolium)) chloride), (PDVIm-Cl), with double anions (Cl^-) and low monomer molecular weight was prepared and utilized in the elimination of anionic dyes (acid orange 7 (AO7), sunset yellow (SY), reactive blue 19 (RB19), congo red (CR)) [32]. Attributed to the mesoporous structure, abundant Cl^- and positively charged imidazole rings, the poly(ionic liquid) (PIL) showed excellent adsorption performance towards anionic dyes; AO7 (1808 ± 84), SY (1022 ± 8), RB19 (2605 ± 254 mg g^{-1}) and CR (6930 ± 196). Studies explored that PDVIm-Cl presented high removal abilities for anionic dyes over a wide pH range (2-10). Moreover, the excellent reusability could be well cleared by the achievable continuous column adsorption-desorption process over three cycle times with the same efficiency.

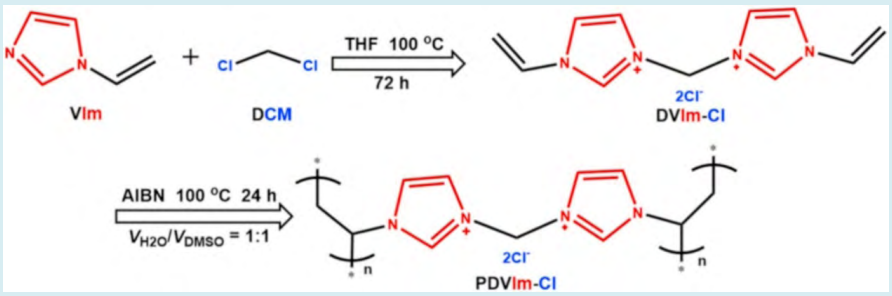

Figure 17: The synthetic route of PDVIm-Cl PIL [32].

Cationic starch enclosed montmorillonite (Mt-CST) adsorbent was investigated [33] for the removal of basic dyes such as; Basic Blue (BB66) and Basic Yellow (BY1) from aqueous solution. Cationic starches (CST) involved ammonium groups with the degree of substitution of 0.16 (CST1) and 0.69 (CST2) were successfully made from the reaction of low molar mass starch with (3-chloro-2-hydroxypropyl trimethyl) ammonium chloride. Finally, a series of Mt-CST nanocomposites were fabricated by controlling the mass ratios of Mt:CST. The results indicated that, the adsorption capacity enhanced with decreasing of cationic groups in the CST or increasing the mass ratios of Mt:CST.

A novel cationic polyelectrolyte microsphere (CCQM) has been prepared using simple chemical crosslinking and emulsification route [34], see Figure 18. CCQM with lower crystallinity, higher specific surface area, pore volume, thermal stability and surface charges, presented adsorption efficiency than pure chitosan microsphere (PCM). These superior functions of CCQM resulted in ultrafast adsorption rate (within 4 min) and ultra-high adsorption capacity to anionic dyes (1500 mg g^{-1} for Congo red (CR) and 179.4 mg g^{-1} for Methyl orange (MO)). The adsorption mechanism could be explained as electrostatic interaction and hydrogen bonding led to the removal of dyes. In addition, excellent recyclability CCQM was achieved (within 10% loss after five cycles). For practical application, the CCQM could be packed in a column to purify wastewater.

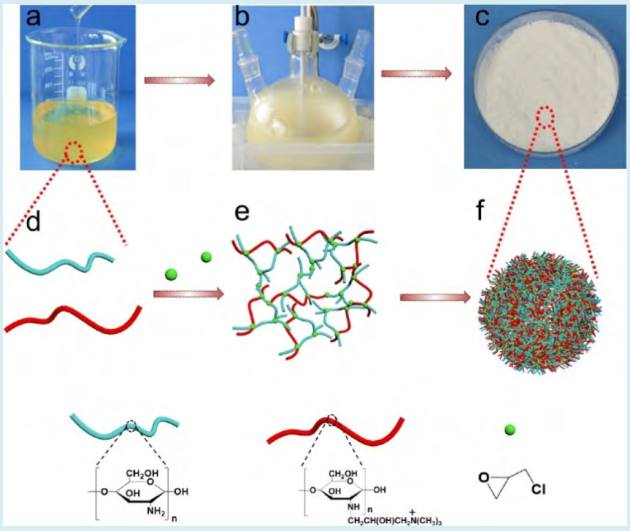

Figure 18: Schematic diagram for the fabrication process of CCQM [34].

Other Polymeric Materials

In the adsorption operation the use of polymeric soluble materials is not a good choice. However, these material must be cross-linked before using, the usefulness of cross–linking agents due to it acting as a chemical binder by entrapment of polymeric function groups hydroxyl (–OH) and amino (–NH_2) groups which may decrease the affinity of the polymer towards the toxic chemicals. Furthermore, some polymeric materials suffer low adsorption efficiency, therefore, a novel crosslinker, filler and functionalization strategies were devoted for enhancement their adsorptive performance.

Hexametaphosphate (Figure 19) was applied as ionic cross-linker for chemically cross-linked of chitosan microsphere (CTS-HMP) as a good non-toxic biosorbent that exhibiting high charge density and thermal stability for adsorption of cationic malachite green (MG) and anionic Reactive Red–195 (RR-195) dyes from aqueous solution [35]. At initial concentration 250 mg L^{-1}, the removal rate gradually increased for MG (69.40 mg) g^{-1} and RR-195 (148 mg g^{-1}) till 100 and 50 min of contact period in a single contaminant system, though the removal efficiency of acid dye was ~2 times higher compared to basic dye under optimum conditions.

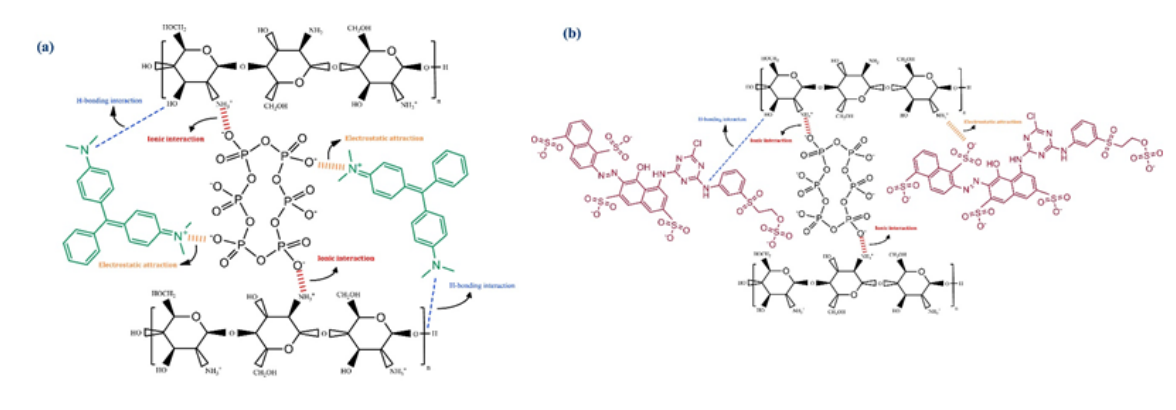

Figure 19: Schematic diagram showing different mechanisms involved in the removal process of MG (a) and RR-195 (b) using chitosan/hexametaphosphate (CTS-HMP) beads [35].

A new nanofiller, citric acid anchored tannic acid (CA-f-TA), was prepared using a simple, economical and green approach as illustrated in Figure 20. The prepared nanofiller was applied in the synthesize of polyethersulfone (PES) nanofiltration (NF) membranes [50]. Referring to the obtained results, the addition of the CA-f-TA nanofiller lead to improve in the pure water flux (PWF), antifouling characters, smoothness and hydrophilicity of membrane surface. Moreover, the composite membrane possesses excellent dye rejection (95.7% for Direct Red 16 (DR 16) and 97% for biologically treated baker's yeast wastewater.

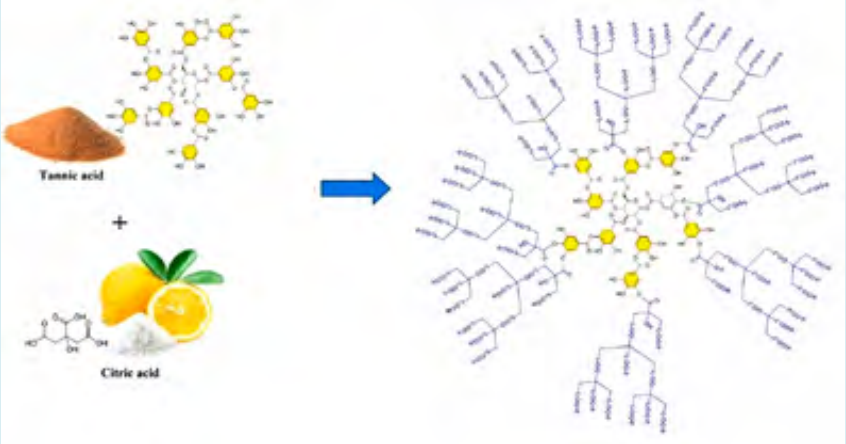

Figure 20: Synthesis of citric acid functionalized tannic acid (CA-f-TA) dendrimer [50].

Three renewable highly efficient adsorbents (M-CS, M-CCL, M-CCSD) (Figure 21) were synthesized from agroforestry residues (corn stalks (CS), Cinnamomum camphora leave (CCL) and Cinnamomum camphora saw dust (CCSD)) by eco-friendly solvent-free esterification with maleic anhydride (MA) for adsorptive elimination of methylene blue (MB) [36]. The three carboxyl-rich adsorbents decontaminated MB rapidly and presented remarkable adsorption activity towards MB reached 870 (M-CS), 741 (M-CCL), 787 (M-CCSD) mg/g according to Langmuir isotherm model. Moreover, the adsorption capacity of M-CS, M-CCL, M-CCSD decreased about 4%, 4%, 3% respectively after 4 desorption-resorption cycles.

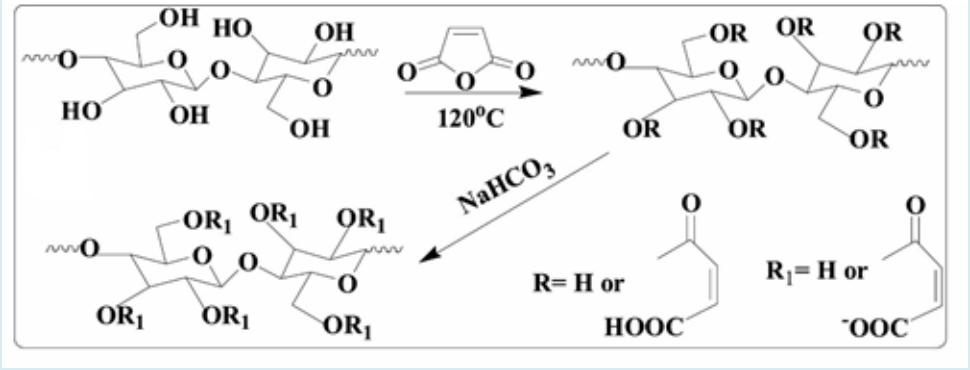

Figure 21: Schematic preparation of maleic modified M-CS, M-CCL, M-CCSD [36].

GO/PNIPAM composite system that has been rationally engineered [37] for elimination of organic dyes from polluted water in a new mechanism, that is, an extraction-like mechanism. The system provides a phase transition to yield a solution phase and a gel phase at temperatures higher than the lower critical solution temperature (LCST) of PNIPAM, at the same time the GO sheets are fully anchored into the gel phase, as presented in Figure 22. More interestingly, dyes can be efficiently adsorbed in the gel phase, thereafter, it can be separated from water in an extraction-like process. Compared to conventional extractive separation systems, the GO/PNIPAM composite system produced two phases yielded by temperature alter, which have a clear phase boundary and are much easier for separation. In addition, the system can save GO from reduction and flocculation so as to retain high stability. PNIPAM and GO can also work synergistically for dye adsorption to give high adsorption capacity and efficiency.

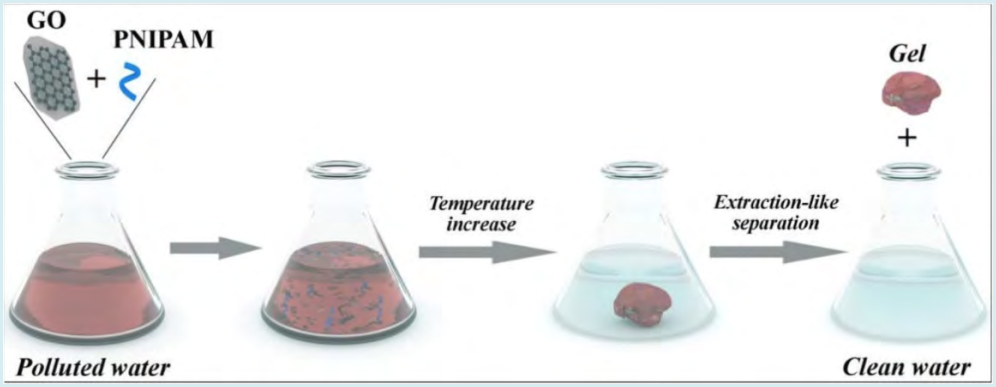

Figure 22: The GO/PNIPAM mixed system can realize temperature-responsive sol–gel transition and remove organic pollutants from water in an extraction-like way [37].

A sulfonated poly (ether ether ketone) (sPEEK) was investigate [51] for adsorption of the methylene blue (MB) and basic violet 16 (BV16) as cationic organic dyes from aqueous solution. The adsorption experiments showed, the composite can remove both cationic dyes with adsorption capacities 98.04 mg g^{-1} for MB, and 181.8 mg g^{-1} for BV16. Furthermore, desorption and recycling studies cleared that the adsorption percent decreased from 99.6% to 99.2%

after the fifth cycle, pointing out sPEEK reusability for MB removal. On the other hand, low desorption percentage of BV16 loaded sPEEK shows that sPEEK may be used for immobilizing of BV16.

A low cost polyvinyl alcohol-glutaraldehyde cross-linked hydrogel beads were fabricated and employed for adsorption of Congo Red dye using batch and fixed-bed reactor [52]. The adsorbent, presented adsorption performance as high as ~34 mg g^{-1}, moreover, these beads could be re-used for 7 times without much variation in removal percent. Batch studies provided a multi-layer adsorption governed by Harkins Jura model. Whereas, the fixed bed experiments revealed steeper break through curves during adsorption operation when high dye influent rates and low bed height were used.

Conclusion

Large quantities of organic dyes wastewater were resulted from industrial activities. The adsorbent based nanomaterials offered an excellent solution for treatment the produced wastewater. Investigating innovative methods for preparation of highly efficient adsorbed nanomaterials that can highly treated the dye contaminants attracted more attention. Superior adsorption efficiency of these materials due to the large surface area, high surface charge densities and surface modification makes them a suitable material to be applied at large scale. Moreover, iron oxide and iron oxide composite nanomaterials have promising adsorption efficiency and excellent separation ability, which are favorable properties for their further application. Moreover, cationic organic polymers were considered a suitable selection in the adsorption of anionic dyes by ion exchange.

References

1. Mauter MS, Zucker I, Perreault F, Werber JR, Kim JH, et al. (2018) The role of nanotechnology in tackling global water challenges. Nat Sustain 1: 166-175.

2. Lu F, Astruc D (2018) Nanomaterials for removal of toxic elements from water. Coordin Chem Rev 356: 147-164.

3. Tabish TA, Memon FA, Gomez DE, Horsell DW, Zhang S (2018) A facile synthesis of porous graphene for efficient water and wastewater treatment. Sci Rep 8: 1817.

4. Jassby D, Cath TY, Buisson H (2018) The role of nanotechnology in industrial water treatment. Nat Nanotechnol 13(8): 670-672.

5. Pourmortazavi SM, Rahimi Nasrabadi M, Aghazadeh M, Ganjali MR, Karimi MS, et al. (2017) Synthesis, characterization and photocatalytic activity of neodymium carbonate and neodymium oxide nanoparticles. J Mol Struct 1150: 411-418.

6. Pourmortazavi SM, Sahebi H, Zandavar H, Mirsadeghi S (2019) Fabrication of Fe_3O_4 nanoparticles coated by extracted shrimp peels chitosan as sustainable adsorbents for removal of chromium contaminates from wastewater: the design of experiment. Compos Part B Eng 175: 107130.

7. Koudehi MF, Pourmortazavi SM (2018) Polyvinyl alcohol/polypyrrole/molecularly imprinted polymer nanocomposite as highly selective chemiresistor sensor for 2,4-DNT vapor recognition. Electroanalysis 30(10): 2302-2310.

8. Khan AA, Kumari S, Chowdhury A, Hussain S (2018) Phase tuned originated dual properties of cobalt sulfide nanostructures as photocatalyst and adsorbent for removal of dye pollutants. ACS Appl Nano Mater 1(7): 3474-3485.

9. Molla A, Sahu M, Hussain S (2016) Synthesis of tunable band gap semiconductor nickel sulphide nanoparticles: rapid and round the clock degradation of organic dyes. Sci Rep 6: 26034.

10. Feng J, Zhu J, Lv W, Li J, Yan W (2015) Effect of hydroxyl group of carboxylic acids on the adsorption of Acid Red G and Methylene Blue on TiO2. Chem Eng J 269: 316-322.

11. Saha B, Das S, Saikia J, Das G (2011) Preferential and enhanced adsorption of different dyes on iron oxide nanoparticles: a comparative study. J Phys Chem C 115(16): 8024-8033.

12. Chowdhury A, Kumari S, Khan AA, Hussain S (2019) Selective removal of anionic dyes with exceptionally high adsorption capacity and removal of dichromate ($Cr_2O_7^{2-}$) anion using Ni-Co-S/CTAB nanocomposites and its adsorption mechanism. J Hazard Mater 385: 121602.

13. Maiti D, Mukhopadhyay S, Devi PS (2017) Evaluation of mechanism on selective, rapid and superior adsorption of Congo red by reusable mesoporous α -Fe2O3 nanorods. ACS Sustain Chem Eng 5: 2-9.

14. Xiong G, Wang B, You L, Ren B, He Y, et al. (2019) Hypervalent silicon-based, anionic porous organic polymers with solid microsphere or hollow nanotube morphologies and exceptional capacity for selective adsorption of cationic dyes. J Mater Chem A 7(1): 393-404.

15. Peng N, Hu D, Zeng J, Li Y, Liang L, et al. (2016) Superabsorbent cellulose-clay nanocomposite hydrogels for highly efficient removal of dye in water. ACS Sustain

Chem Eng 4(12): 7217-7224.

16. Tian P, Han XY, Ning GL, Fang HX, Ye JW, et al. (2013) Synthesis of porous hierarchical MgO and its superb adsorption properties. ACS Appl Mater Interfaces 5(23): 12411-12418.

17. Muthukumaran T, Philip J (2021) Synthesis of water dispersible phosphate capped $CoFe_2O_4$ nanoparticles and its applications in efficient organic dye removal. Colloids and Surfaces A: Physicochemical and Engineering Aspects 610: 125755.

18. Shair AS, Abo Dena AS, El Sherbiny IM (2021) Matrix-dispersed PEI-coated SPIONs for fast and efficient removal of anionic dyes from textile wastewater samples: Applications to triphenylmethanes. Spectrochimica Acta Part A: Molecular and Biomolecular Spectroscopy 249: 119301.

19. Lei C, Wen F, Chen J, Chen W, Huang Y, et al. (2021) Mussel-inspired synthesis of magnetic carboxymethyl chitosan aerogel for removal cationic and anionic dyes from aqueous solution. Polymer 213: 123316.

20. Hu C, Le AT, Pung SY, Stevens L, Neate N, et al. (2021) Efficient dye-removal via Ni-decorated graphene oxide-carbon nanotube nanocomposites. Materials Chemistry and Physics 260: 124117.

21. Arasi MA, Salem A, Salem S (2021) Production of mesoporous and thermally stable silica powder from low grade kaolin based on eco-friendly template free route via acidification of appropriate zeolite compound for removal of cationic dye from wastewater. Sustainable Chemistry and Pharmacy 19: 100366.

22. Raza S, Wen H, Peng Y, Zhang J, Li X, et al. (2021) Fabrication of SiO_2 modified biobased hydrolyzed hollow polymer particles and their applications as a removal of methyl orange dye and bisphenol-A. European Polymer Journal 144: 110199.

23. Guo RF, Zhao X, Li XY, Liu ZH (2021) Preparation and formation mechanism of graphene oxide supported hollow mesoporous $Mg_2Si_3O_6(OH)_4$ micro-nanospheres with highly efficient methylene blue dye removal from wastewater. Colloids and Surfaces A: Physicochemical and Engineering Aspects 610: 125936.

24. Kumari S, Khan AA, Chowdhury A, Bhakt AK, Mekhalif Z, et al. (2020) Efficient and highly selective adsorption of cationic dyes and removal of ciprofloxacin antibiotic by surface modified nickel sulfide nanomaterials: Kinetics, isotherm and adsorption mechanism. Colloids and Surfaces A: Physicochemical and Engineering Aspects 586: 124264.

25. Yu CX, Chen J, Zhang Y, Song WB, Li XQ, et al. (2021) Highly efficient and selective removal of anionic dyes from aqueous solution by using a protonated metal-organic framework, Journal of Alloys and Compounds 853: 157383.

26. Ahlawat W, Katari N, Dilbaghi N, Hassan AA, Kumara S, et al. (2020) Carbonaceous nanomaterials as effective and efficient platforms for removal of dyes from aqueous systems. Environmental Research 181: 108904.

27. Vigneshwaran S, Sirajudheen P, Nikitha M, Ramkumar K, Meenaksh S (2021) Facile synthesis of sulfur-doped chitosan/biochar derived from tapioca peel for the removal of organic dyes: Isotherm, kinetics and mechanisms. Journal of Molecular Liquids 326: 115303.

28. Dolunay D, Koyuncu E, Okur M (2021) Removal of AV 90 dye using ordered mesoporous carbon materials prepared via nanocasting of KIT-6: Adsorption isotherms, kinetics and thermodynamic analysis. Separation and Purification Technology 257: 117657.

29. Deng F, Liang J, Yang G, Huang Q, Dou J, et al. (2021) Direct generation of poly(ionic liquids) on mesoporous carbon via Diels–Alder and multicomponent reactions for ultrafast adsorptive removal anionic organic dye with high efficiency. Journal of Environmental Chemical Engineering 9(1): 104872.

30. Feng M, Yu S, Wu P, Z Wang, Liu S, et al. (2021) Rapid, high-efficient and selective removal of cationic dyes from wastewater using hollow polydopamine microcapsules: Isotherm, kinetics, thermodynamics and mechanism. Applied Surface Science 542: 148633.

31. Bao J, Li H, Xu Y, Chen S, Wang Z, et al. (2021) Multi-functional polyethersulfone nanofibrous membranes with ultra-high adsorption capacity and ultra-fast removal rates for dyes and bacteria. Journal of Materials Science & Technology 78: 131-143.

32. Lin J, Su T, Chen J, Xue T, Yang S, et al. (2021) Efficient adsorption removal of anionic dyes by an imidazolium-based mesoporous poly(ionic liquid) including the continuous column adsorption-desorption process. Chemosphere 272: 129640.

33. Lawchoochaisakul S, Monvisade P, Siriphannon P (2021) Cationic starch intercalated montmorillonite nanocomposites as natural based adsorbent for dye removal. Carbohydrate Polymers 253: 117230.

34. Cai L, Ying D, Liang X, Zhu M, Lin X, et al. (2021) A novel

cationic polyelectrolyte microsphere for ultrafast and ultra-efficient removal of heavy metal ions and dyes. Chemical Engineering Journal 410: 128404.

35. Raval NP, Mukherjee S, Shah NK, Gikas P, Kumar M (2021) Hexametaphosphate cross-linked chitosan beads for the eco-efficient removal of organic dyes: Tackling water quality. Journal of Environmental Management 280: 111680.

36. Tang Y, Lin T, Jiang C, Zhao Y, Ai S (2021) Renewable adsorbents from carboxylate-modified agro-forestry residues for efficient removal of methylene blue dye. Journal of Physics and Chemistry of Solids 149: 109811.

37. Cao M, Shen Y, Yan Z, Wei Q, Jiao T, et al. (2021) Extraction-like removal of organic dyes from polluted water by the graphene oxide/PNIPAM composite system. Chemical Engineering Journal 405: 126647.

38. Li ZJ, Sun YK, Xing J, Meng A (2019) Fast removal of methylene blue by Fe_3O_4 magnetic nanoparticles and their cycling property. J Nanosci Nanotechnol 19(4): 2116-2123.

39. Li JX, Jiang BQ, Liu Y, Qiu CQ, Hu JJ, et al. (2017) Preparation and adsorption properties of magnetic chitosan composite adsorbent for Cu^{2+} removal. J Clean Prod 158: 51-58.

40. Cruz JC, Nascimento MA, Luciano VA, Souza FC, Oliveira JWV, et al. (2021) A novel method to synthesize iron oxide nanomaterials: Characterization, properties, and performance on the direct red 80 dye removal from aqueous solution. Ceramics International 47: 4357-4360.

41. Wang J, Zhang Q, Shao X, Ma J, Tian G (2018) Properties of magnetic carbon nanomaterials and application in removal organic dyes. Chemosphere 207: 377-384.

42. Farhadi S, Mahmoudi F, Amini MM, Dusek M, Jarosova M (2017) Synthesis and characterization of a series of novel perovskite-type $LaMnO_3$/Keggin-type polyoxometalate hybrid nanomaterials for fast and selective removal of cationic dyes from aqueous solutions. Dalton Trans 46(10): 3252-3624.

43. Abdellaha AR, Abdelhamidb HN, El Adasya AB AAM, Atallaa AA, Aly KI (2020) One-pot synthesis of hierarchical porous covalent organic frameworks and two-dimensional nanomaterials for selective removal of anionic dyes. Journal of Environmental Chemical Engineering 8(5): 104054.

44. Lee H, Dellatore SM, Miller WM, Messersmith PB (2007) Mussel-inspired surface chemistry for multifunctional coatings. Science 318(5849): 426-430.

45. Liebscher J, Mrowczynski R, Scheidt HA, Filip C, Hadade ND, et al. (2013) Structure of polydopamine: a never-ending story? Langmuir 29(33): 10539-10548.

46. Kang S, Baginska M, White SR, Sottos NR (2018) Core-shell polymeric microcapsules with superior thermal and solvent stability. ACS Appl Mater Interfaces 7(20): 10952-10956.

47. Cui KX, Yan B, Xie YJ, Qian H, Wang XG, et al. (2018) Regenerable urchin-like Fe3O4@PDA-Ag hollow microspheres as catalyst and adsorbent for enhanced removal of organic dyes. J Hazard Mater 350: 66-75.

48. Hu Y, Yue M, Yuan F, Yang L, Chen C (2021) Bio-inspired fabrication of highly permeable and anti-fouling ultrafiltration membranes based on bacterial cellulose for efficient removal of soluble dyes and insoluble oils. Journal of Membrane Science 621: 118982.

49. Katarzyna Jankowska, Adam Grzywaczyk, Adam Piasecki, Ewa Kijeńska Gawrońska, Luong N Nguyen, et al. (2021) Electrospun biosystems made of nylon 6 and laccase and its application in dyes removal. Environmental Technology & Innovation 21: 101332.

50. Rahimi Z, Zinatizadeh AA, Zinadini S, Loosdrecht M (2021) A hydrophilic and antifouling nanofiltration membrane modified by citric acid functionalized tannic acid (CA-f-TA) nanocomposite for dye removal from biologically treated baker's yeast wastewater. Journal of Environmental Chemical Engineering 9(1): 104963.

51. Hızal J, Kanmaz N, Yılmazoğlu M (2021) Adsorption efficiency of sulfonated poly (ether ether ketone) (sPEEK) as a novel low-cost polymeric adsorbent for cationic organic dyes removal from aqueous solution. Journal of Molecular Liquids 322: 114761.

52. Jain P, Sahoo K, Mahiy L, Ojh H, Trivedi H, et al. (2021) Color removal from model dye effluent using PVA-GA hydrogel beads. Journal of Environmental Management 281: 111797.